Journal of Visualization, Vol. 2, No. 1 (1999) 31-36

Three-phase Flow Pattern Recognition in Horizontal Pipelines using Electrical Capacitance Tomography

Corlett, A. E.*

* National Engineering Laboratory, East Kilbride, Glasgow, UK.

Received 25 January 1999.
Revised 23 April 1999.

***Abstract*:** An experimental study was performed to evaluate the suitability of using an electrical capacitance tomography (ECT) system to visualise three component mixtures of crude oil, water and gas. The performance of the ECT system was examined over a range of three-phase flow conditions and regimes. The flow visualisations from the tomography system were compared with the images filmed using a CCD camera aligned with a Perspex pipe section. Results indicated that ECT was most successful in flow pattern identification for low water fraction flows. However, slug and stratified regimes could be identified for high water fraction flows. A critical factor in the quality and reliability of the generated image was the image reconstruction scheme used.

***Keywords*:** electrical capacitance tomography, three-phase flow.

1. Introduction

The flow of oil, water and gas within a pipeline in two and three component combinations is more complex than that of a single phase. A wide range of patterns form which are determined by the relative ratios of gas and liquid and the velocities of each phase relative to the other (e.g. Barnea and Taitel, 1986; Hewitt and Hall Taylor, 1970). For two-phase flows such as oil/gas and water/gas in a horizontal pipeline, the patterns formed can be broadly categorised into four distinct regimes: stratified, slug, annular and bubble flow (refer to Fig. 1). Addition of a third phase can lead to an increase in the standard regimes due to the separation of oil and water; examples being slug-separated and slug-dispersed flows (Hall, 1997).

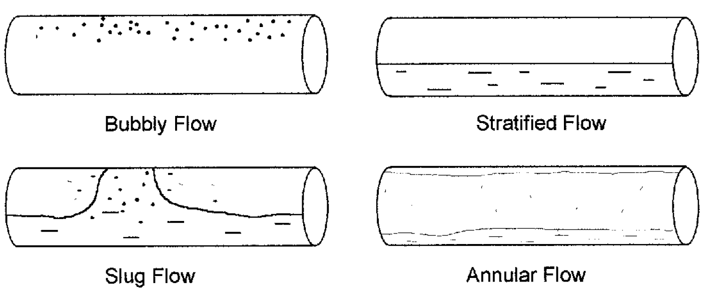

Fig. 1. Horizontal two-phase flow patterns.

Three-phase flows are inherently difficult to visualise and current instrumentation can provide only limited information. Real-time visualisation of these gas/liquid distributions is of particular interest to the oil industry for use in evaluations that link flow conditions with multiphase meter performance.

Electrical capacitance tomography (ECT) uses the variations of electrical permittivity within a test section to generate an image of the dielectric distribution.It is a non-intrusive and real-time technique which is ideally suited to visualising two component flows in which there is a difference in permittivities. A system generally consists of a sensor, a capacitance measuring unit and a control system, the sensor being a number of capacitance electrodes wrapped around the area to be imaged. The capacitance between all combinations of each pair of electrodes is measured. These values are then used to generate, via reconstruction algorithms, an image of the pipe contents. The theory and design of ECT systems are detailed in various papers, for example Huang et al. (1989) and Isaksen et al. (1994). The various reconstruction and analysis techniques available are discussed in Beck et al. (1995).

In general, ECT systems are not suited to imaging high water content flows (Hammer et al, 1998). This is because water, being highly conductive, has a tendency to short out the electrodes. Other methods such as electrical resistance tomography or electrical impedance tomography should be used in preference for such flows. Similarly, basic ECT systems can only differentiate between two phases, generally between the liquid and the gas. To image a third phase an additional sensor is needed (e.g. Johansen et al., 1995).

Given the diversity of multiphase flows it would appear to be necessary to use a combination of techniques to highly accurately image such flows (Ceccio and George, 1996). However, in an industrial situation this is not always viable. Hence, the purpose of this study was to examine the use of a single, commercially available ECT system to visualise the flow within a multiphase pipeline and to determine its reliability in distinguishing the various liquid/gas flow regimes.

2. ECT System

The study used a commercial ECT system (PTL, UK) with a specifically designed sensor head. The sensor consisted of twelve, 5.08 cm long, electrodes with driven guard electrodes to increase axial resolution. ECT system choice and design are discussed in Corlett (1997).

Two image reconstruction packages were included in the system software. The 'on-line' scheme was a Linear Back Projection algorithm (e.g. Xie et al., 1991). Images could be reconstructed 'off-line,' using an iterative scheme (Yang et al., 1997).

3. Experimental Procedure

The investigation was performed in the UK National Multiphase Flow Facility. The test fluids were crude oil, magnesium sulphate solution and nitrogen. The test section diameter was 101.6 mm and the length 60 m. A Perspex spool piece was placed approximately 0.6 m upstream of the sensor head, enabling the flow within the test section to be videotaped using a CCD camera. Although the videotape recording was not simultaneous with the ECT data collection, the flow conditions were sufficiently stable for any comparisons to be valid.

The test programme encompassed stratified, slug, annular and bubble flow regimes. For two phases, oil/gas and water/gas were used, whilst for three phase flows the water fraction was varied between 5% and 90%. The test temperature was 40 ;.

The ECT system had to be calibrated before use with the sensor head filled with the baseline conditions of first high and then low permittivity substances. Calibrations for all tests used oil/gas or water/gas combinations.

4. Results

4.1 Flow Regimes

(1) Stratified flow

Figure 2(a) shows an image of a stratified two-phase oil/gas flow. An oil layer (red) can be seen in the bottom of the pipe with gas (blue) in the upper section. This compares well with the visualisation using the Perspex section in which there was a clear definition between the two layers. The red marks on the upper pipe surface are system anomalies and will be discussed in Section 5.

The image of a stratified water/gas flow (Fig. 2(b)) represents also the equivalent visualisation using the CCD camera. However, in this case, the liquid layer is less well defined than in Fig. 2(a) and incorporates both a red and green layer. Since red corresponds to the highest measured permittivity (100% liquid) and blue to the lowest (100% gas), green corresponds to values in between. That is, it signifies areas in which the system cannot resolve completely the difference between liquid and gas.

(2) Slug flow

Figure 3 illustrates the evolution of a slug within the test section for an oil/gas flow. The frames are separated by 0.015 s. As the slug approaches, the level of the liquid within the pipe increases until eventually the whole of the pipe is filled. After a flowrate dependent time interval, the liquid layer decreases to a base level of approximately 50% of the pipe diameter.

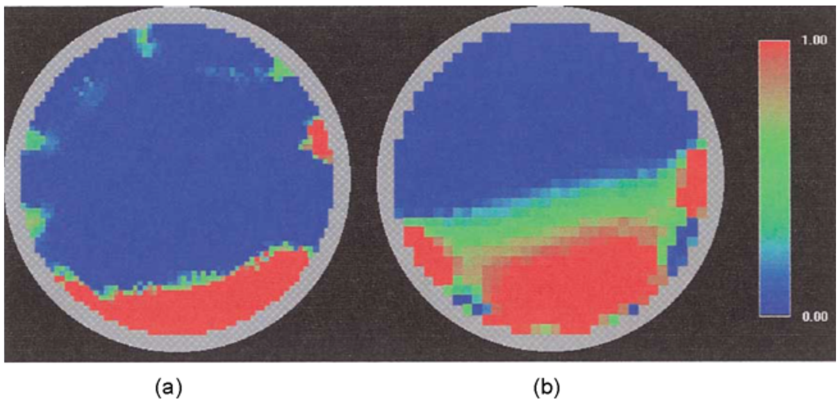

Fig. 2. Stratified flow : (a) oil/gas (iterated), (b) water/gas (on-line).

Since visibility within the Perspex section could be severely restricted during some oil/gas slug flows, the ECT system often had a distinct advantage over the CCD camera.

The ECT system was able to distinguish the various forms of slug flow, the relative flow velocities, slug lengths and frequencies. Absolute measures of velocity were not possible since this would have required a second sensor head linked into the data acquisition system.

Slug flows could be distinguished at all water fractions even if the formation and dissolution were not so clearly defined as in Fig. 3. As the mixture water fraction increased, the distinction between layers of liquid and gas became less clear, however the presence of a slug of liquid within the sensor could always be determined.

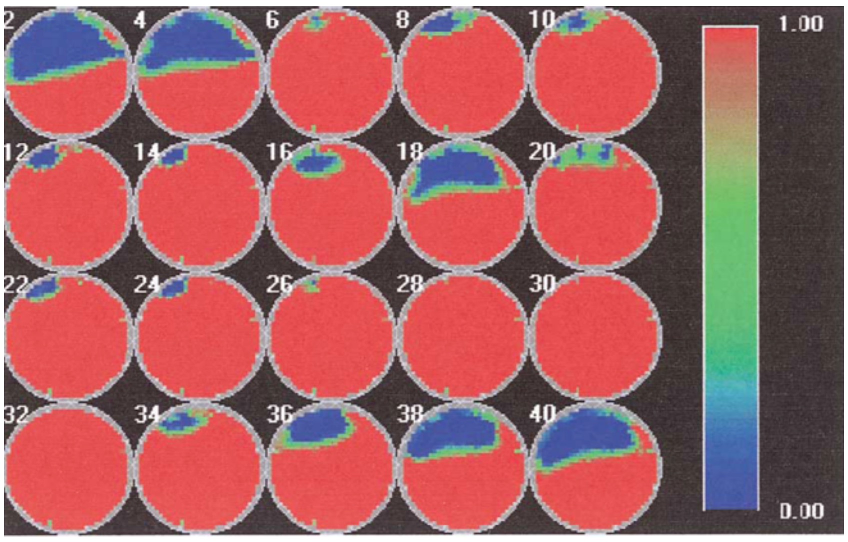

Fig. 3. Frames from an oil/gas slug flow (iterated reconstruction).

(3) Annular flow

Flow pattern recognition was less straightforward with annular flow. Figure 4(a) shows an example of the visualisation achieved with an oil/gas flow. Although this image is similar to that of a stratified flow, when viewed in real-time on-line, the overall flow behaviour differed significantly. The images tended to flicker more than with stratified or slug flows. In addition, the on-line images contained more green than was found generally with a stratified/slug flow. In this case, the green areas probably would have corresponded to areas of aerated liquid. Only low water fraction annular flows could be visualised using the ECT system.

(4) Bubble flow

Bubble flow was not investigated as fully as other flow regimes, since bubble flow only occurs at the limit of the maximum liquid flowrate in the NEL facility. However, an example of a bubble flow image from an oil/gas flow is shown in Fig.4(b).

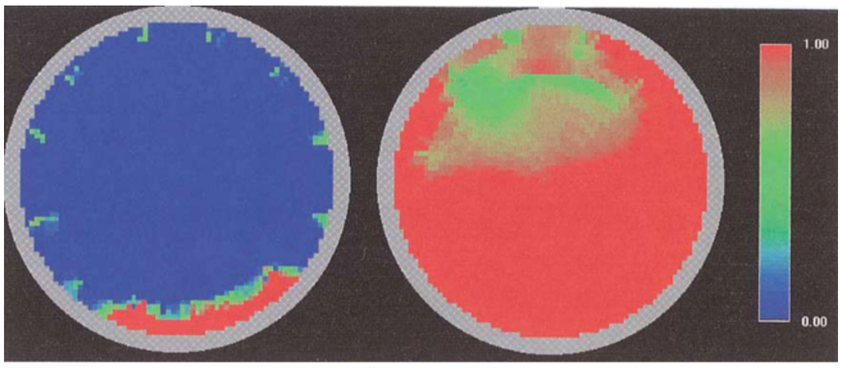

(a) (b)

Fig. 4. (a) Annular oil/gas flow (iterated), (b) Bubble oil/gas flow (iterated).

In this image there is a patch of green surrounded by red. This corresponds to areas of gas or highly aerated liquid (green) within a liquid (red). When viewed on-line, bubble flow tended to appear like this image with the green patches flickering within the red surround. As with annular flow, only low water fraction bubble flows could be visualised using the ECT system.

4.2 Calibration Effects

For flows with water fractions up to approximately 50%, the oil/gas calibration was used. The water/gas combination did not produce images which correlated with those visible through the Perspex section. This is illustrated by Fig. 5, which is the on-line response to the two calibrations for a 50% water fraction flow. Comparing Fig. 5(a) and 5(b), the oil/gas and water/gas calibrations respectively, it can be seen that although the basic distribution of liquid is the same for both, the one resulting from the oil/gas calibration is more clearly defined. As the water fraction increased above 50%, the oil/gas calibration became less effective in correctly differentiating the areas of high and low permittivity, whilst the water/gas calibration became more effective.

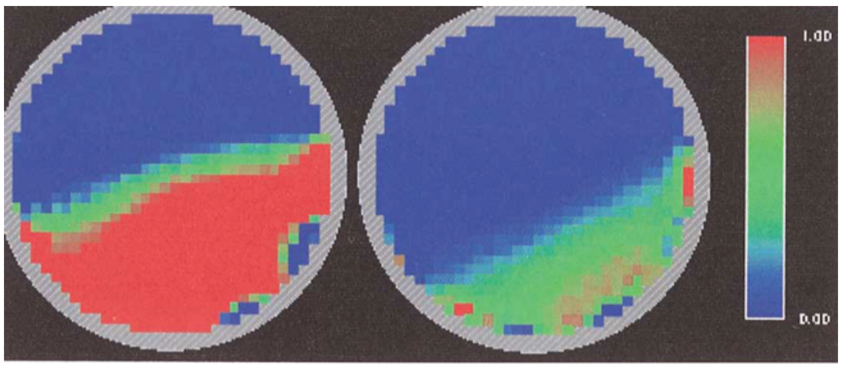

(a) (b)

Fig. 5. Slug flow; 50% water fraction (on-line): (a) oil/gas calibration, (b) water/gas calibration.

4.3 Image Reconstruction Effects

Post-processing of frames allowed comparison between these iterated images and the on-line, LBP images. For two-phase oil/gas flows and low water fraction three-phase flows, the difference between the images was simply that the iterated ones had a better resolution. This agreement did not occur with high water fraction flows.

Figure 6 shows images taken during slug flow at a water fraction of 75%. Both images correspond to the same frame with Fig. 6(a) and 6(b) being the on-line and off-line images respectively. The slug is not fully within the sensor section and so the cross-section is not completely filled with liquid. Nonetheless there is still a high level of liquid within the pipe and Fig. 6(a) is a good representation of the visualisation through the Perspex section. The iterated image is not a good representation of the true flow. The image suggests that there are gaseous regions on the lower pipe walls and liquid regions on the upper walls. Results such as these meant that for three-phase flow mixtures with water fractions above approximately 50%, only the on-line reconstruction scheme could be relied upon to give a physically realistic image of the pipe contents.

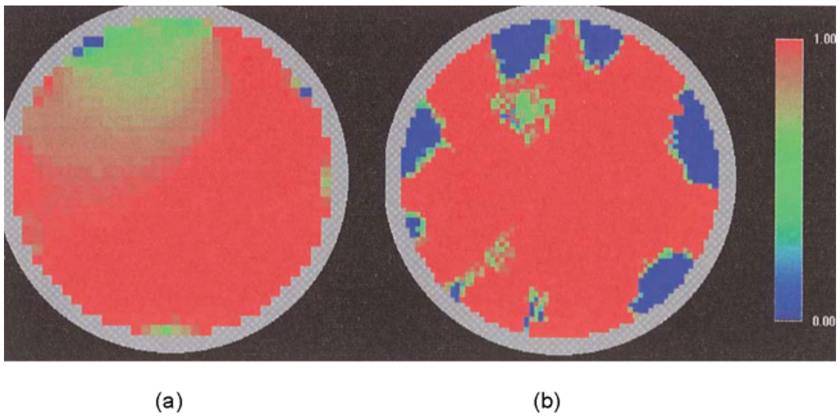

Fig. 6. Slug flow; 75% water fraction: (a) on-line, (b) off-line.

5. Discussion

Overall, the tomographic system images matched those observed using the CCD camera. The resolution and quality of results varied with water fraction and system calibration.

Anomalous marks tended to appear in some images if the iterated reconstruction algorithm was used and were more numerous for high water fraction flows. As illustrated by Fig. 6, for such flows the iterated image was not an accurate representation of the often visible behaviour in the pipeline. This suggests that the effect was aggravated by the increasing presence of water.

The majority of anomalies were found on the pipe walls and in positions which appeared to correlate with those of the electrodes. For an electric field the region closest to a capacitance sensor is the most sensitive to changes in permittivity. This is because an electric field is a 'soft field' which means that the field itself is distorted by the presence of dielectric material. Sensitivity maps, built in to the software, are used to compensate for these effects. A small error in a sensitivity coefficient can lead to large errors in the reconstructed image. Even the cumulative effect of a number of small errors in the sensitivity map could have a significant effect on the accuracy of the produced image. Similarly these maps are also used to compensate for the potential effect of water shorting out some electrodes. If the supplied map does not adequately reflect the true electrode behaviour this again could lead to errors in the reconstructed image. A quantifiable indication that the iterated reconstruction algorithm was not suitable for use with water/gas flows was the capacitance error value. This value appeared on-screen as the iteration program was executed. For oil/gas flows the capacitance error decreased with number of iterations until reaching a constant value, whereas for water/gas flows this error remained constant.

6. Conclusions

The imaging results using the ECT system compared well with those from the CCD camera. For oil/water mixtures with water fractions up to approximately 50%, the most successful results were achieved when the system was calibrated with oil and gas. On-line image reconstruction produced images which matched those visualised through the Perspex pipe section and the majority of flow regimes could be recognised easily. In some cases, particularly at high velocities, the tomography system was able to visualise flow behaviour which was not apparent when using the CCD system. Off-line imaging using the iterative reconstruction algorithm resulted in improved image resolution and quality.

When the mixture water fraction increased to above 50%, water/gas system calibrations were necessary. The on-line, LBP images continued to be reliable. Stratified and slug flow patterns remained easily recognisable, however others such as annular became less so. Image reconstruction using the iteration algorithm became increasingly unreliable with obvious erroneous pixels becoming increasingly prominent. These anomalies were considered to be due to soft field effects.

Thus, the results show that electrical capacitance tomography can be used as a flow visualisation tool for multiphase flows, but for high water fraction flows such systems should be used in conjunction with other techniques.

Acknowledgments

The work described in this paper was funded by the Flow Programme of the UK Department of Trade and Industry.

References

Barnea, D. and Taitel, Y., Flow Pattern Transitions in Two Phase Gas-Liquid Flows, Encyclopaedia of Fluid Mechanics, 3(1986), 403-474.

Beck, M. S., Hoyle, B. S., Morris, M. A., Waterfall, R. C. and Williams, R. A., Process Tomography- Implementation for Industrial Processes, (1995), University of Manchester Institute of Science and Technology.

Ceccio, S. L. and George, D. L., A Review of Electrical Impedance Techniques for the Measurement of Multiphase Flows, J. Fluids Engineering, 118, (1996), 391-399.

Corlett, A. E., Portable Real-Time Tomographic Instrument, NEL Report 041/97, (1997).

Hall, A. R. W., Flow Patterns in Three-phase Flows of Oil, Water and Gas., Proceedings of Multiphase '97 (Cannes), (1997).

Hammer, E . A, Johansen, G . A. and Thorn, R., Measurement Principles in Multiphase Metering- Their Benefits and Limitations, Proceedings of the Fourth International Conference - Multiphase Technology Series (London), (1998).

Hewitt, G. F. and Hall Taylor, N. S., Annular Two-Phase Flow, (1970), Pergamon Press.

Huang, S. M., Plaskowski, A. B., Xie, C. G. and Beck, M. S., Tomographic Imaging of Two-Component Flow using Capacitance Sensors, J. Phys. E: Sci. Instrum., 22 (1989), 173-177.

Isaksen, O. and Nordvedt, J. E., A New Reconstruction Algorithm for Process Tomography., Meas. Sci. Technol., 4 (1993), 1464-1474.

Johansen, G . A., Froystein, T., Hjertaker, B. T., Isaksen, O., Strandos, S. K., Skoglund, T. O., Abro., E. and Hammer, E. A., The Development of a Dual Mode Tomograph for Three-component Flow Imaging, Chemical Engineering Journal, 56 (1995), 175-182.

Xie, C. G., Huang, S. M., Hoyle, B. S. and Beck, M. S., Tomographic Imaging of Industrial Equipment - Development of System Model and Image Reconstruction Algorithm for Capacitance Tomography, Proceedings of the Fifth Conference on Sensors and their Applications (Edinburgh), (1991), 203-208.

Yang, W. Q, Gamio, J. C. and Beck, M. S., A Fast Iterative Image Reconstruction Algorithm for Capacitance Tomography, Proceedings of the Eighth Conference on Sensors and their Applications (Glasgow), (1997), 47-52.

Author's Profile

Anne E. Corlett: She gained her BSc Honours degree in Physics from Durham University (UK) in 1992. She was awarded a PhD in Physics from the University of Edinburgh in 1997 for work on vortex shedding at low Reynolds numbers. Since joining the National Engineering Laboratory she has worked in the Multiphase area, investigating such flow behaviour as the viscosity of crude oil and water mixtures and the quantification of dissolved gas in oil. She is currently using Laser Doppler velocimetry to study the flow measurement implications of installation effects on ultrasonic meters.